Check for updates

A hydrazide organogelator for fluoride sensing with hyperchromicity and gel-to-sol transition†

Sangwoo Park,‡[a] Jeewon Ju,‡[b] Young Ju Lee‡*[a] and Sang-Yup Lee (ID) ‡*[b]

Sensing of fluoride in a solvent is highly required in healthcare and environmental rehabilitation. Among the various sensing methods, optical sensing has attracted significant research interest because it can conveniently recognize fluoride. Herein, a low molecular weight organogelator, $N'1,N'6$-bis(3-(1-pyrrolyl) propanoyl) hexanedihydrazide (DPH), containing a central butyl chain conjugated to two pyrrole rings through hydrazide groups, was used for optical sensing of fluoride in the forms of both solution and organogel. Association of fluoride with the −NH moiety of the hydrazide group endowed the DPH solution in dimethylformamide with a hyperchromicity under 350 nm. Exploiting the UV absorptivity, the DPH solution was examined as a chemosensor, displaying good selectivity toward fluoride among various anions and moderate sensitivity with a detection limit of 0.49 μM. The practical use of the DPH solution was demonstrated for fluoride sensing in toothpaste. Binding of fluoride also changed the molecular interactions of the DPH organogel, resulting in a phase transition from gel to sol. This gel-to-sol transition enabled the sensing of fluoride by the naked eye.

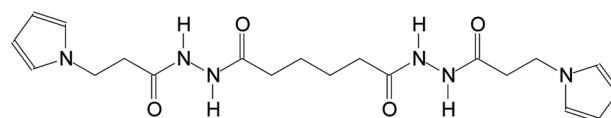## 1 Introduction

Fluoride regulates many physiological and biochemical functions in nature and is commonly utilized as an ingredient for dental-care products and water treatment.[1–3] However, excess intake of or long-term exposure to fluoride can cause fatal complications including skeletal fluorosis, osteoporosis, and damage to the liver, lungs, and other organs.[4–7] Thus, the selective sensing of fluoride among various anions is required for environmental rehabilitation applications and medical diagnostics. Various techniques have been explored for sensing fluoride; these include spectrophotometry, ion-exchange chromatography, and electrochemistry.[8] These techniques offer a high fluoride-sensing accuracy, but they require costly instruments, thereby complicating the development of economic and portable sensors. Specifically, a sensor material whose physicochemical properties can be examined by the naked eye should be beneficial because it is straightforward and does not require expensive instruments.[9] In previous studies,

various fluoride sensing molecules containing both chromophore and receptor motifs for color or fluorescence emission and recognition of fluoride, respectively, were developed. For instance, anthracene,[10,11] anthraquinone,[12,13] calixpyrrole,[14,15] dipyrrolylquinoxaline,[16] and other chromophore molecules have been used as chromogenic units, displaying various colors and/or fluorescence. In addition, fluoride-binding motifs such as urea,[17,18] thiourea,[19,20] hydrazide,[21,22] indole,[23,24] and imidazole[23,25] groups have been adopted for selective recognition of fluoride. The receptor groups mostly recognize fluoride by H-bonding or deprotonation of the −NH moiety.

In addition to these molecular probes, molecular assemblies have been explored for fluoride sensing. Compared to molecular chemosensor probes, these supramolecular assemblies are advantageous for manipulation and observation by the naked eye because they can achieve a phase transition along with color/fluorescence changes. With low molecular weight chromogenic derivatives, some fluoride-sensitive self-assembled organogels have been prepared that exhibit photochromic changes.[21,26–33] Recently, self-assemblies of $N'1,N'6$-bis(3-(1-pyr-rolyl)propanoyl)hexanedihydrazide (hereafter referred to as DPH, Scheme 1) were reported to form discrete rod-like

[a]Korea Basic Science Institute Gwangju Center, 300 Yongbong-dong, Buk-gu, Gwangju, 61186, Republic of Korea. E-mail: yjlee@kbsi.re.kr; Fax: +82-62-530-0519; Tel: +82-62-712-4413

[b]Department of Chemical and Biomolecular Engineering, 50 Yonsei-ro, Seodaemun-gu, Seoul, 03722, Republic of Korea. E-mail: leessy@yonsei.ac.kr; Fax: +82-2-312-6401; Tel: +82-2-2123-5758

‡ S. P. and J. J. designed and performed the experimental work. Y. L. performed the NMR study and discussed the results. S. L. analyzed the data and prepared the manuscript. All authors discussed and commented on the manuscript.

Scheme 1   Molecular structure of $N'1,N'6$-bis(3-(1-pyrrolyl)propanoyl) hexanedihydrazide (DPH).

structures with abnormal photosensitizing activity.[34] Exploiting the photosensitizing activity of DPH assemblies hybridized with ionic or organic chromophores, the optical sensing of target organic molecules were realized.[34,35] DPH could also form an organogel when self-assembled in select organic solvents such as a mixture of DMF and chloroform. The organogel contains a network of self-assembled nanofibers containing a large amount of organic solvent.[35] This network structure can be disassembled by disturbing the molecular structure and potentially used for the development of a phase-transition material that can be activated by external stimuli.

Herein, optical sensing of fluoride was demonstrated using a DPH solution and organogel. The DPH molecule exhibited high selectivity toward fluoride over various anions because of the capability of the hydrazide group to recognize fluoride. The UV absorbance intensity increased as the fluoride concentration increased owing to the deprotonation of the hydrazide bond. Exploiting this hyperchromic effect, the sensing of fluoride in toothpaste was demonstrated using the prepared DPH solution. Furthermore, the gel-to-sol phase transition of the DPH organogel when exposed to fluoride was demonstrated, which enabled the visual sensing of fluoride without a need for additional costly instrumentation. The molecular interaction between fluoride and the hydrazide bond of DPH was supported by ^{1}H-NMR spectroscopy data, and a reaction mechanism was proposed.

2 Experimental

2.1 Chemicals and DPH synthesis

The 1-(2-cyanoethyl) pyrrole (99%, Sigma-Aldrich) and adipic acid dihydrazide (AAD, 98%, Sigma-Aldrich) served as the pyrrole source and alkyl chain spacer, respectively; they were used as the main chemicals for DPH synthesis. These chemicals were conjugated *via* carbodiimide chemistry using *N,N'*-dicyclohexylcarbodiimide (DCC; 99%, Sigma-Aldrich) and *N*-hydroxysuccinimide (NHS; 97%, Sigma-Aldrich) as conjugating agents. Potassium hydroxide (KOH; Duksan Sci. Corp.) was used for hydrolysis of the intermediate product. Dimethylsulfoxide (DMSO; 99%, Sigma-Aldrich), *N,N*-dimethylformamide (DMF; 99.5%, Duksan Sci. Corp.), and chloroform (99%, Duksan Sci. Corp.) were used as organic solvents for the synthesis of DPH and preparation of the DPH organogel. Tetra-*n*-butylammonium (TBA) salts with various anions (F^-, Cl^-, Br^-, I^-, BF_4^-, ClO_4^-, NO_3^-, and PF_6^-) were chosen as anion sources and were dissolved in DMF (2 mM). These TBA salt solutions were diluted to the desired concentrations immediately prior to spectroscopic analysis.

DPH synthesis was conducted according to a previously reported protocol.[36] Briefly, 1-(2-cyanoethyl) pyrrole was converted to 1-(2-carboxyethyl)pyrrole (Py-COOH) *via* hydrolysis with KOH solution under reflux. The Py-COOH carboxyl group was conjugated with the amine group of AAD *via* formation of hydrazide bonds through the DCC/NHS conjugation reaction; DCC and NHS were added to the Py-COOH solution in DMSO to activate the carboxyl group; next, AAD was added to initiate the conjugation reaction at room temperature. The synthesized

DPH molecules were dissolved in DMSO while precipitating the dicyclohexylurea byproduct. The byproduct was filtered, and subsequent cooling of the DMSO solution generated powdery DPH precipitates. Synthesis scheme is illustrated in ESI (Fig. S1†).

2.2 Characterization

The synthesized Py-COOH and DPH molecule were confirmed using multinuclear ^{1}H-NMR, ^{13}C-NMR spectroscopy (500 MHz, Propulse, Agilent, USA) and high-resolution mass spectroscopy (Synapt G2-Si HDMS, WATERS). ^{1}H NMR data of Py-COOH is as follows: δ 2.85 (m, 2H); 4.24 (m, 2H); 6.03 (m, 2H-CH of pyrrole); 6.69 (m, 2H-CH of pyrrole); 10.69 (bs, H-OH of carboxyl). ^{1}H NMR data of DPH is as follows: δ 1.51 (m, 4H); 2.11 (m, 4H); 2.59 (m, 4H); 4.14 (s, 4H); 5.95 (m, 4H-CH of pyrrole); 6.71 (m, 4H-CH of pyrrole). ^{13}C NMR data of Py-COOH is as follows: δ 172.53, 120.54, 107.61, 44.46, 36.12. ^{13}C NMR data of DPH is as follows: δ 170.83, 168.72, 120.53, 107.60, 44.50, 35.38, 32.91, 24.66. Chloroform-d (δ = 7.26) was used as a solvent for Py-COOH and DMSO-d_6 (δ = 2.50) was used as a solvent for DPH in NMR spectroscopy. High-resolution mass spectroscopy (HRMS) of Py-COOH calculated for $C_7H_{10}NO_2$: 140.0712. Found: 140.0710 [M]$^+$ APCI (ASAP+). HRMS of DPH calculated for $C_{20}H_{28}N_6O_4$: 416.2172. Found: 417.2247 [M + H]$^+$ ESI (ASAP+). The ^{1}H-NMR, ^{13}C-NMR and mass spectroscopy were shown in the ESI (Fig. S2–7†).

2.3 UV-vis spectroscopy of DPH-anion interactions

Selective detection of fluoride was achieved using a UV-vis spectrophotometer (U-3501, Hitachi, Japan). To 1 mL of the DPH solution (1 mM) in DMF, 1 mL of TBA salt solution (2 mM) with different anions was added. After 1 min of mixing, the UV-vis spectrum of the DPH and TBA salt mixture was recorded. In addition, the molecular interaction of anions with DPH molecules was investigated *via* ^{1}H-NMR spectroscopy using a 500 MHz NMR instrument.

2.4 Preparation of the DPH solution and organogel

DMF, a polar aprotic solvent, was used to prepare the DPH solution for use as a chemosensor. Note that DPH was soluble only to the selected solvents of DMF and DMSO. The DPH organogel was prepared by inducing the self-assembly of DPH molecules upon addition of non-polar organic solvents. To prepare the organogel, the DPH solution in DMF (20 mM) was prepared as a stock solution. Subsequently, chloroform was added to the DPH solution to prepare a chloroform-rich mixture at a volumetric ratio of 1 : 9 (DMF : chloroform). The final DPH concentration in the organogel was 2 mM. The morphologies of the DPH fibril assemblies were observed from the DPH xerogel using scanning electron microscopy (SEM; SU-70, Hitachi, 15 kV).

3 Results and discussion

3.1 Fluoride sensing using the DPH solution

Using the DPH solution in DMF as a fluoride chemosensor, fluoride sensing was performed. First, the capability of DPH to sense fluoride was tested. As shown in Fig. 1a, the DPH solution
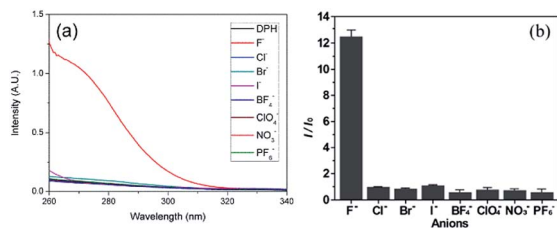
Fig. 1 UV-vis absorption intensity of DPH in the presence of various anions. (a) UV-absorbance spectra of a DPH solution (0.1 mM) in DMF with various anions. A single equivalent fluoride to DPH corresponds to two moles of fluoride per one mole of DPH based on the presence of two hydrazide groups in a single DPH molecule. (b) Bar graph representing the change of relative absorbance intensities of DPH at 275 nm after addition of various anions (I_0: intensity of the original DPH solution).

Fig. 2 Changes of UV-vis absorbance with increasing fluoride concentration. (a) Increasing absorbance intensity at 275 nm with increasing fluoride concentration (0–10 equiv., 0.5 equiv. intervals) at room temperature (inset: UV-vis spectra of the DPH solution). (b) Responses of DPH solution to the stepwise addition of fluoride at various concentrations.

in DMF did not show intrinsic absorbance peaks under $\lambda = 320$ nm in the UV region. Upon addition of fluoride (i.e. tetrabutylammonium fluoride ($[CH_3(CH_2)_3]_4NF$) solution) to the DPH solution, a significant hyperchromic effect with broad UV absorption was observed, whereas other TBA salts containing anions such as Cl^-, Br^-, I^-, BF_4^-, ClO_4^-, NO_3^-, and PF_6^- did not show any noticeable change. This hyperchromic effect in the UV-vis spectra is indicative of new DPH-fluoride complex formation. Considering that hydrogen-bonding donor motifs have been used as fluoride receptors, the hydrazide groups in DPH are putative recognizing segments for fluoride.[21,22,37] The selectivity of DPH to fluoride is high enough to display ca. 12-fold enhanced absorption intensity at $\lambda = 275$ nm after the addition of 5 equiv fluoride over those of other anions (Fig. 1b). For further investigation into the selectivity of DPH toward fluoride, the sensing interference by other anions was examined. In the presence of other anions at the same concentration (5.0 equiv.), selectivity toward fluoride was not significantly altered (ESI, Fig. S8†). These results indicate that the DPH molecule recognizes fluoride exclusively, thereby demonstrating its capability as a selective chemosensor.

Quantitative analysis of the sensitivity of DPH to fluoride was conducted by monitoring the UV absorbance change at 275 nm with stepwise addition of 0.5 equiv. fluoride to a 0.1 mM DPH solution. Upon the addition of fluoride, the absorption intensity increased linearly until 2 equiv. fluoride with a sensitivity of 0.23 equiv^{-1} (46 μM^{-1}; Fig. 2a). Further addition of fluoride resulted in a moderate increase in the absorption intensity, eventually reaching a plateau. The linear increase in absorption intensity is advantageous for fluoride sensing at low concentrations (<2 equiv.) with considerable sensitivity. From the linear region, the limit of detection was estimated to be 0.49 μM using the 3σ method. This limit of detection in the DPH solution is comparable to those of other molecular fluoride sensors (Table S1†), and is enough to detect the WHO (World Health Organization) acceptable limit of the fluoride concentration (79 μM) in drinking water.[38] The response time was evaluated by addition of fluoride at various concentrations (Fig. 2b). The DPH solution responded to fluoride quickly (<1 min), and the UV absorbance remained constant before the further addition
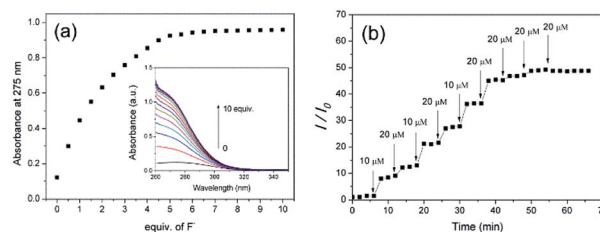
of fluoride in a stepwise manner. This quick response to fluoride is beneficial for real-time sensing. It must be noted that the stepwise changes demonstrate that 10 μM fluoride is recognizable by the DPH molecules; this is sufficient for the sensing of 1.5 ppm (79 μM) fluoride, which is the maximum permissible limit in drinking water.[23]

To prove the practical applicability of the DPH solution as a chemosensor, the fluoride content in toothpaste was examined. Commercially available toothpaste (Colgate®) was dissolved in DMF at a concentration of 1 mg mL^{-1}, and the solution was centrifuged to remove solid components. The obtained toothpaste supernatant was added to the DPH solution, and the UV absorbance intensity was measured to determine the fluoride concentration. The measured fluoride concentration of the toothpaste was 57.8 μM, which corresponds to a 9.5% deviation from the stated fluoride content of the product (52.8 μM; Fig. S9†). Given the intra-product differences of toothpastes, this deviation is acceptable.

3.2 Analyses of DPH-fluoride binding

To analyze the selective recognition of fluoride by DPH, the binding stoichiometry and molecular interactions of fluoride with DPH were surveyed. First, a Benesi–Hildebrand plot was drawn from the UV absorbance values measured at various fluoride concentrations (Fig. 3a). Interestingly, the normalized intensity of $1/(A - A_0)$ exhibited the best linear correlation with the reciprocal of $[F^-]^{1.5}$ ($R^2 = 0.999$), instead of the reciprocals of $[F^-]$ or $[F^-]^2$, implying complex formation between DPH and fluoride at a 1 : 1.5 ratio (Fig. S10†). This non-integer ratio of complex formation was further confirmed by the Job's plot shown in Fig. 3b. The maximum absorbance of the DPH-fluoride complex was observed at $[F^-]/[F^-] + [DPH] = 0.6$, corresponding to $[DPH] : [F^-] = 1 : 1.5$. This non-integer molar ratio clearly differs from the 1 : 2 stoichiometry expected from the molecular structure of DPH containing two hydrazide groups.[21] The unique non-integer molar ratio of the DPH-fluoride complex is plausible, considering that the stoichiometric analyses were performed at the equilibrium state of complexation. Not every hydrazide group binds to fluoride at equilibrium, although two possible binding sites are present in a single DPH molecule.
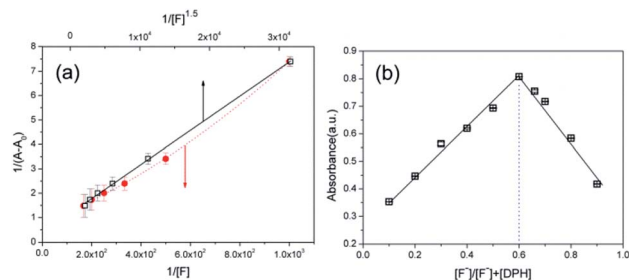
Fig. 3 Stoichiometry of DPH–fluoride complexation. (a) Benesi–Hildebrand plot of DPH-fluoride complex formation. [F⁻] is the concentration of fluoride in units of mol L⁻¹ [M]. (b) Job's plot of the DPH-fluoride complex. The concentration of [DPH] + [F⁻] maintained at 1.5 mM.

Subsequently, ^{1}H-NMR titration experiments were conducted to examine the molecular interaction between DPH and fluoride. The chemical shifts of the hydrazide N–H protons of native DPH were evident at $\delta = 9.7$ and $\delta = 9.8$ ppm (Fig. 4). These peaks disappeared upon the addition of 1.0 equiv. fluoride due to the formation of the N–H···F⁻ hydrogen bonds. After the addition of 2.0 or higher equiv. fluoride, spectral up-field shifts of methylene and pyrrolic protons were observed, inducing significant shielding of the methylene protons adjacent to the amide. These peak shifts are indicative of the delocalization of negative charge over the entire molecule due to deprotonation. Meanwhile, with 2.0 equiv. fluoride, triplet peaks appeared at $\delta = 16.1$ ppm, clearly demonstrating the formation of HF₂⁻.[21] Therefore, it can be inferred that hydrogen bonds between fluoride and hydrazide N–H developed at lower fluoride concentration, and further addition of fluoride resulted in hydrazide deprotonation to produce HF₂⁻.

Based on the reported fluoride-hydrazine binding mechanism,[21] the addition of fluoride was expected to facilitate the isomeric transformation of the *anti* to *syn* conformation of DPH by forming hydrogen bonds with –NH, a proton receptor in the hydrazide moiety (Fig. S11†).[39] Increased fluoride concentration may result in deprotonation of the hydrazide group, producing
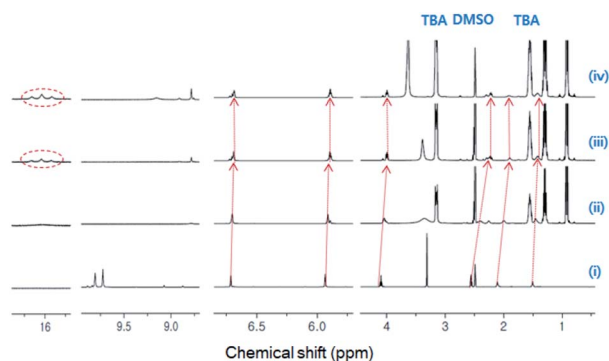
HF₂⁻ whose triplet ^{1}H-NMR peaks were observed at $\delta = 16.1$ ppm. Concurrently, the deprotonated hydrazide group likely attracted neighboring carbonyl oxygens, thereby leading to the isomeric transformation of DPH.

3.3 Fluoride sensing by the DPH organogel

DPH molecules self-assemble to form organogels in the DMF-chloroform mixture. As described in the experimental section, an opaque DPH organogel was produced from the DPH solution in DMF by gradual addition of chloroform to form a chloroform-rich environment (v/v = 1 : 9). The assembly of DPH molecules was driven by intermolecular forces that are affected by solvent polarity. With increasing non-polar solvent content, the DPH molecules are self-organized to form fibrous assemblies that are driven by both the hydrogen bonding[35] and the binding interactions between pyrrole rings that are driven by polarization and London dispersion forces.[40] Organogels are advantageous over solutions owing to the ease of manipulation and naked-eye sensing of fluoride upon phase transfer from the gel to sol. To observe the microstructure of the DPH organogel, the solvents were freeze-dried to produce a DPH xerogel. Like other organogels, the DPH xerogel adopted a network structure connected with nanofibers (Fig. 5). The curved fibers, with *ca.* 50 nm diameter, were connected with each other to form a porous structure with submicron-sized pores. The DPH organogel remained stable in the vial for over a month without deterioration and did not flow even when inverted (Fig. 6a).

Degelation, accompanying the phase transition from gel to sol occurred when excessive fluoride was added to the organogel. Upon addition of 10 equiv of the powdery tetrabutylammonium fluoride salt to the top of the organogel, a thin layer of transparent solution was produced. This transparent solution progressively expanded; eventually, all the organogel was transformed into a transparent solution (Fig. 6a). This process required approximately 5 min. Degelation implies that the self-organization of the DPH molecules was interrupted by fluoride that presumably disrupted the hydrogen bonds and/or the pyrrole ring interactions. In addition, isomeric transformation is a likely mechanism underlying degelation, resulting in the disassembly of the fibrous DPH assembly. The gel-to-sol transition was observed by the naked eye; it was applicable for the development of a solid, low-cost sensor for detecting fluoride.

The selectivity of the organogel for fluoride was examined by applying other tetrabutylammonium anion salts. Only the
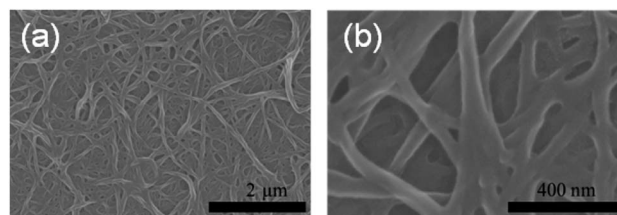

Fig. 4 The ^{1}H NMR spectra of DPH (2.0×10^{-2} M) in DMSO-d₆ bound with different amounts of fluoride (left: magnified spectra at $\delta = 16.1$ ppm). From (i) to (iv), the added amount of fluoride were 0, 1, 2, and 3 equiv., respectively.

Fig. 5 FE-SEM images of the prepared DPH xerogel at (a) low and (b) high magnifications.
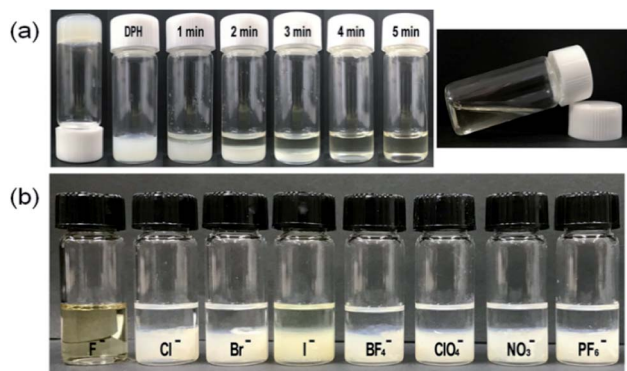
Fig. 6 Photos of the gel-to-sol phase transition of the DPH organogel (5 mg mL^{-1}). (a) Progress of degelation over time after the addition of tetra-butylammonium fluoride (TBAF) powder (10 equiv.). (b) Selective phase transition of the DPH organogel toward fluoride and various anions.

tetrabutylammonium fluoride fully transformed the opaque organogel into a light yellowish transparent solution; other anions did not change the organogel (Fig. 6b). These results, which are congruent with previous results of the DPH solution, verified that the organogel can selectively recognize fluoride.

4 Conclusions

In summary, the optical and visible sensing of fluoride was systematically studied by exploiting the hyperchromicity and phase transition of DPH. The organogelator composed of DPH exhibited considerable sensitivity for fluoride over other anions owing to the selective binding of hydrazide that acted as a recognition motif. Fluoride formed hydrogen bonds with –NH of the hydrazide group, resulting in high selectivity and further deprotonation of the hydrazide group in DPH. As a consequence of deprotonation, the internal charge transfer with conformation change resulted in hyperchromaticity and phase transition, allowing for the optical and/or visible sensing of fluoride. The gel-to-sol transition of the DPH organogel upon fluoride addition demonstrated their potential use as a low-cost fluoride sensor that can be recognized by the naked eye without costly instrumentation. The dual responses of DPH toward fluoride with short response time, considerable sensitivity, and outstanding selectivity are advantageous for use in a chemosensor for health care and environmental rehabilitation applications.

Conflicts of interest

There are no conflicts to declare.

Acknowledgements

Notes and references

1 D. Kanduti, P. Sterbenk and B. Artnik, *Mater Sociomed*, 2016, **28**, 133–137.

2 E. A. Martínez-Mier, *Alternative Med.*, 2011, **17**, 28–32.

3 S. Jagtap, M. K. Yenkie, N. Labhsetwar and S. Rayalu, *Chem. Rev.*, 2012, **112**, 2454–2466.

4 A. A. Mohammadi, M. Yousefi, M. Yaseri, M. Jalilzadeh and A. H. Mahvi, *Sci. Rep.*, 2017, **7**, 17300.

5 X. Xiong, J. Liu, W. He, T. Xia, P. He, X. Chen, K. Yang and A. Wang, *Environ. Res.*, 2007, **103**, 112–116.

6 E. V. Thrane, M. Refsnes, G. H. Thoresen, M. Låg and P. E. Schwarze, *Toxicol. Sci.*, 2001, **61**, 83–91.

7 M. S. Kurdi, *Indian J. Anaesth.*, 2016, **60**, 157–162.

8 N. Ameer, G. Mustafa, I. Khan, M. Zahid, M. Yasinzai, S. Shahab, N. Asghar, I. Ullah, A. Ahmad, I. Munir, H. Khan, S. Badshah, I. Shahid, M. N. Ahmad, A. Zia and S. Ahmad, *Fluoride*, 2018, **51**, 252–266 and references therein.

9 N. Kaur, G. Kaur, U. A. Fegade, A. Singh, S. K. Sahoo, A. S. Kuwar and N. Singh, *Trends Anal. Chem.*, 2017, **95**, 86–109.

10 B. Uttam, H. M. Chawla, N. Pant and M. Shahid, *J. Photochem. Photobiol., A*, 2017, **349**, 224–229.

11 W. Huang, H. Lin, Z. Cai and H. Lin, *Talanta*, 2010, **81**, 967–971.

12 P. M. Reddy, S.-R. Hsieh, C.-J. Chang and J.-Y. Kang, *J. Hazard. Mater.*, 2017, **334**, 93–103.

13 E. Kim, H. J. Kim, D. R. Bae, S. J. Lee, E. J. Cho, M. R. Seo, J. S. Kim and J. H. Jung, *New J. Chem.*, 2008, **32**, 1003–1007.

14 A. F. Danil De Namor, I. Abbas and H. H. Hammud, *J. Phys. Chem. B*, 2007, **111**, 3098–3105.

15 M. Nemati, R. Hosseinzadeh, R. Zadmard and M. Mohadjerani, *Sens. Actuators, B*, 2017, **241**, 690–697.

16 C.-Y. Wu, M.-S. Chen, C.-A. Lin, S.-C. Lin and S.-S. Sun, *Chem.–Eur. J.*, 2006, **12**, 2263–2269.

17 M. Mohar and T. Das, *Colloid Interface Sci. Commun.*, 2019, **30**, 100179.

18 X. Wu and Q. Niu, *Sens. Actuators, B*, 2016, **222**, 714–720.

19 A. Misra, M. Shahid and P. Dwivedi, *Talanta*, 2009, **80**, 532–538.

20 M. G. Murali, K. A. Vishnumurthy, S. Seethamraju and P. C. Ramamurthy, *RSC Adv.*, 2014, **39**, 20592–20598.

21 X. Ran, Q. Gao and L. Guo, *RSC Adv.*, 2017, **7**, 56016–56022.

22 Y. Zhang, X. Yang, G. Sun, H. Zhang, X. Liu, F. Zhu, S. Qin, Z. Zhao and Y. Cui, *Spectrochim. Acta, Part A*, 2018, **199**, 161–169.

23 A. Jain, R. Gupta and M. Agrawal, *Synth. Commun.*, 2017, **47**, 1307–1318.

24 D. Jeyanthi, M. Iniya, K. Krishnaveni and D. Chellappa, *Spectrochim. Acta, Part A*, 2015, **136**, 1269–1274.

25 H. Liu, B. Zhang, C. Tan, F. Liu, J. Cao, Y. Tan and Y. Jiang, *Talanta*, 2016, **161**, 309–319.

26 X. Cao, N. Zhao, H. Lv, A. Gao, A. Shi and Y. Wu, *Sens. Actuators, B*, 2018, **266**, 637–644.

27 X. Yu, D. Xie, Y. Li, L. Geng, J. Ren, T. Wang and X. Pang, *Sens. Actuators, B*, 2017, **251**, 828–835.

28 J. Sivamani and A. Siva, *Sens. Actuators, B*, 2017, **242**, 423–433.

29 C. Pati and K. Ghosh, *Supramol. Chem.*, 2019, **31**, 732–744.

30 A. Panja, S. Ghosh and K. Ghosh, *New J. Chem.*, 2019, **43**, 10270–10277.

31 C. Pati and K. Ghosh, *New J. Chem.*, 2019, **43**, 2718–2725.

32 S. Ghosh, K. Goswami and K. Ghosh, *Supramol. Chem.*, 2017, **29**, 946–952.

33 K. Ghosh and C. Pati, *Tetrahedron Lett.*, 2016, **57**, 5469–5474.

34 S. Park and S.-Y. Lee, *Sens. Actuators, B*, 2014, **202**, 690–698.

35 S. Park and S.-Y. Lee, *Sens. Actuators, B*, 2015, **220**, 318–325.

36 S. Park, T.-G. Kwon, S.-I. Park, S. Kim, J. Kwak and S.-Y. Lee, *RSC Adv.*, 2013, **3**, 8468–8473.

37 L. S. Evans, P. A. Gale, M. E. Light and R. Quesada, *New J. Chem.*, 2006, **30**, 1019–1025.

38 X.-Y. Kong, L.-J. Hou, X.-Q. Shao, S.-M. Shuang, Y. Wang and C. Dong, *Spectrochim. Acta, Part A*, 2019, **208**, 131–139.

39 B. Bai, J. Ma, J. Wei, J. Song, H. Wang and M. Li, *Org. Biomol. Chem.*, 2014, **12**, 3478–3483.

40 T. Sieranski, *Struct. Chem.*, 2016, **27**, 1107–1120.